Available online at www.sciencedirect.com
ScienceDirect
Applied Geochemistry 22 (2007) 2334–2343
Applied Geochemistry
www.elsevier.com/locate/apgeochem

Tomographic radiotracer studies of the spatial distribution of heterogeneous geochemical transport processes

Marion Gründig [a,*], Michael Richter [a], Anita Seese [b], Osama Sabri [b]

[a] *Institut für Interdisziplinäre Isotopenforschung, Permoserstr. 15, D-04318 Leipzig, Germany*
[b] *Universität Leipzig, Klinik und Poliklinik für Nuklearmedizin, Stephanstr. 11, D-04103 Leipzig, Germany*

Received 25 July 2006; accepted 5 April 2007
Editorial handling by Dr. P. McMahon
Available online 9 June 2007

Abstract

Within the scope of the further development of geochemical transport models the consideration of the influence of the heterogeneous structures of the geological layers plays an important role. For the verification and parameter estimation of such models it is necessary to measure the heterogeneous transport and sorption processes inside the samples. Tomographic radiotracer methods (positron emission tomography (PET)) enable nondestructive spatially resolved observations of the transport processes in these layers. A special quantitative evaluation system for geoscientific PET studies was developed. Investigations of the water flow distribution in a drill core of a lignite mining dump and of the migration of Cu ions in a horizontal soil column illustrate the potential of this method. Spatial distribution functions of the flow velocity, the specific mass flow and the longitudinal dispersivity were determined on the basis of PET investigations.

1. Introduction

The heterogeneous pore space of soils and sediments and the fracture structure of rocks influence water flow and transport of contaminants and colloids. Because the flow velocity, solute concentrations, hydrodynamic parameters and geochemical adsorption and kinetic parameters cause spatial distributions, which are controlled by the framework of the pores and fractures, within the scope of the further development of geochemical transport models the connection of pore space and the transport process plays an important role. Recently methods have become available to measure pore distribution more accurately. The use of transmission computer tomography (CT) has been reported for the characterization of pore space in soils and sediment cores (Bayer et al., 2004; Kastel et al., 2000; Vogel et al., 1999). For the determination of surface interactions in the pore space the effective interface and the exact velocity are needed to determine accurate equilibrium and kinetic parameters. Besides CT and nuclear magnetic resonance tomography (MRT) (Nestle et al., 2003a; Oswald et al., 1997) positron emission tomography (PET) is suited to image nondestructively the spatial distribution of water flow and solute concentrations within a drill core or a soil column (Degueldre et al., 1996; Ogilvie et al., 2001;

* Corresponding author. Fax: +49 341 2352731.
E-mail address: gruendig@iif-leipzig.de (M. Gründig).

0883-2927/$ - see front matter © 2007 Elsevier Ltd. All rights reserved.
doi:10.1016/j.apgeochem.2007.04.024

Richter et al., 2000). PET is a nondestructive diagnostic technique where a positron emitting radionuclide labelled radiotracer is injected via the flow input of a laboratory device for the investigation of the transport processes in the sample. A PET-Scanner is used to record the distribution of the radioactive nuclei in the sample. Imaging is obtained by means of two 511 keV gamma quanta which are emitted almost collinearly when a positron emitted from the tracer annihilates an electron in the surrounding matter. Two opposite detection crystals detect the two gamma quanta in coincidence. The location of the emitting tracer nuclide is positioned on the connecting line between these detectors. By measuring with several detector pairs at different angles a tomographic image reconstruction can be executed. The use of radionuclides enables tomographic measurements in a region of very low concentrations which cannot be studied with other tomographic methods. The spatial resolution is in the order of 1–5 mm dependent on the available PET-Scanner. Such an elementary volume (voxel) of $5 \times 5 \times 5$ cm^3 containing several pores is the representative elementary volume (REV) for many transport models basing on Darcy's law. Therefore it has been used also in several MRT investigations (Deuerer and Vogeler, 2004; Oswald et al., 2002).

MRT has a better spatial resolution ($\approx$1 mm) but it demands much higher tracer concentrations and the interpretation of the signals is sometimes not well-defined in a complex geological matrix if the water molecules are not only adsorbed by the tracer ions but also by the solid matrix (Hall et al., 1997). In many cases the geological materials enclose paramagnetic components which affect MRT measurements negatively or make them impossible (Nestle et al., 2002; Van As and Van Dusschoten, 1997). Artificial porous media (glass beds, pure quartz sand) are studied in most cases. Special low field devices can diminish these effects but they demand significantly longer measuring times. Therefore PET studies are an important complement to MRT. It is the only method to carry out tomographic flow investigations over a broad concentration profile including very low concentrations in the range of 10^{-9} mol/L.

Some investigations using PET are known to visualize stationary flow paths in porous media (Degueldre et al., 1996; Ogilvie et al., 2001). In this work dynamic tracer experiments are explained making possible the determination of the spatial distributions of several flow parameters.

The use of PET investigations for the validation and further development of geochemical transport models demanded the development of a special quantitative evaluation system of the PET images. The fundamental scheme of this evaluation system is explained. Several proposals are given (Richter, 2002) for the quantitative evaluation of PET images regarding geochemical modelling. Studies of the distribution of the water flow in a vertical soil column containing an undisturbed drill core of a lignite mining dump and of the transport of Cu ions in a horizontal column filled with sand demonstrate the great potential of PET for the modelling of heterogeneous mass transfer processes in geological layers.

2. Experimental

A special PET-Scanner (GEO-PET) was developed with optimum results for geoscientific PET investigations (Richter et al., 2000). This device needs a measuring time of several hours for one scan of the sample. It can be used only for the investigation of slow transport processes. In the following examples relatively fast processes were studied which demand shorter measuring times (300 s). Therefore the measurements were carried out with the commercial PET camera ECAT EXAT HR$^+$/CTI Siemens, which was developed for medical purposes, at the University of Leipzig. The available spatial resolution amounts to about 5 mm.

2.1. Investigation of the drill core of the lignite mining dump

A vertical soil column (polyethylene tube, diameter 10.5 cm, height 56 cm) contained an undisturbed drill core taken from a lignite mining dump in Cospuden (former lignite mine in the south of Leipzig) at a depth of 11 m. The material consisted of fine sand, silt, gravel, stones and small coal. The average material density of the core was 2.3 g/cm^3. The water content of the core was 40.4 vol.%. Further investigations of geochemical reactions which are connected with the increase of the groundwater level are planned in this column.

The PET experiments were carried out under saturated conditions after adjustment of stationary flow conditions. The specific flow rate (water input/column cross section) in the column was 0.002 cm/s.

The radiotracer ([^{18}F]KF, 600 MBq, 0.1 M KF) was injected in the shape of an impulse. ^{18}F was produced by irradiation of a water target enriched with

^{18}O with protons at the cyclotron (Cyclone 18/6) of the FZ Rossendorf. The conservative hydrodynamic behaviour of this tracer was demonstrated in batch tests with the original soil material. The F^- tracer is absorbed insignificantly and can be used for hydrodynamic studies similarly to Br^-.

After injection of the tracer into the column the spatial concentration distribution was measured with the PET camera at intervals of 5 min in several cross sections of the column.

2.2. Investigation of the transport of copper ions in a horizontal soil column

The horizontal soil column (Fig. 1) was filled with sand (grain size 100–500 μm, organic C not detectable) and operated under saturated flow conditions generated by a non-pulsating pump. In this column a horizontal groundwater flow was simulated. Analogous measurements were done with magnetic resonance tomography (MRT) at the TU München. Ceramic filters on the in- and output distribute even flow in the cross section. The injection of the tracer was carried out in the middle of the column to prevent wall flow in the entrance section.

2.2.1. Production of the tracer solution

^{64}Cu ($T_{1/2} = 12.7$ h, $\beta^+ = 17.9\%$) was produced by irradiation of Cu powder with thermal neutrons in the research reactor BER II of the Hahn-Meitner-Institut Berlin. Cu yield (4 mg) to an activity of 650 MBq after a time of irradiation of 24 h at a flux of 10^{13} n/cm^2 s. The Cu powder was dissolved in 1 mL 1 M HNO_3, evaporated and taken up in 3 mL water, which results in a tracer concentration of 0.02 mol/L $Cu(NO_3)_2$.

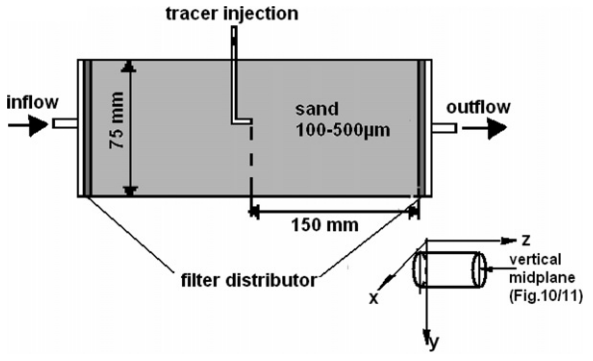

Fig. 1. Horizontal soil column.

2.2.2. Experiment

For comparison purposes, the Cu experiment used the same concentration and flow conditions as the MRT experiments of Nestle et al. (2003a,b). In theory, lower tracer concentrations could be used in PET studies.

The column was arranged horizontally in the centre of the object field of the PET-camera. The input water flow was 22 cm^3/min (specific flow rate: water input/column cross section = 0.0083 cm/s). The pH-value of 6 was constant during the experiment. After 30 min the tracer solution (3 mL) was injected and the first tracer distribution was measured 80 s after the injection. After this the tracer concentration distribution was measured at intervals of 120 s. After 480 s the water supply was closed and an elution solution of 0.01 M KNO_3 was fed in and three further measurements at intervals of 120 s were carried out. In addition the residence time distribution was measured with the tracer KBr detected by conductivity.

3. Estimation of model parameters

3.1. Evaluation system for geoscientific PET studies

The result of the tomographic reconstructions of the measured primary data in PET studies is a stack of images. Each image contains the information of one cross section in a device specific format. The general standard format DICOM was developed to compare the images of different devices (Clunie, 2000). The header of a DICOM data set contains the information about the number of pixels in x- and y-direction, the scaling factor (mm/pixel), the number of images in the stack and the distance (pixels) between two neighbouring cross sections. The density value of each pixel is characterized by an 8-bit or 16-bit number (selectable data format: little or big endian). The software package of modern PET cameras contains a module to convert the data into the DICOM format. DICOM is used as input format in several image analysis programmes. After conversion into DICOM format the data set is imported into the image analysis system "Scion Image" developed by the National Institute of Health and Scion Corporation (Rasband and Bright, 1995). This system enables a 3-D-reconstruction of the tracer concentration distribution and the calculation of stacks of axial sections. Several colour maps can be used to convert grey scale images into colour images. A lot of special macros can be

integrated into the system to realize the extraction of quantitative values for several demands. Stacks can be combined to make a video of the tracer concentration distribution during the transport process. Density values can be extracted automatically for special areas in different images or the whole stack. Several methods can be used to divide the cross section into area elements. Several parameters can also be extracted for selected density intervals. For all selections the quantitative parameter sets can be exported as tables. These data are used to calculate the spatial distribution functions of transport parameters of the geochemical transport models. The spatial moments M_i can be calculated with the mean density values.

3.2. Calculation of the spatial velocity distribution from the concentration ratios in 2 cross sections

The results of PET measurements are spatially resolved tracer concentration distributions in a particular cross section of the sample. For modelling of transport processes the spatial distribution of the flow velocity is required. For that the determination of the tracer concentration distribution in two neighbouring cross sections (distance Δz) at two times $(t, t+\Delta t)$ is sufficient to calculate the velocity distribution (Fig. 2).

The mean flow velocity v in the segment $F_{x,y}$ of the cross section can be calculated with special values of the tracer distribution function $\Phi_{x,y}(z,t)$ which are determined from the pixel values $(A_{i,j})$ of tomographic images.

The spatial velocity distribution in all cross section elements can be calculated based on the one-dimensional dispersion model

$$\Phi_{x,y}(z,t) = \frac{K}{\sqrt{\sigma(t)}} \exp - \frac{(z-vt)^2}{\sigma(t)} \tag{1}$$

$$\sigma(t) = 4D \cdot t \tag{2}$$

$$K = \frac{A_0}{F \cdot \sqrt{\pi}}$$

with D = dispersion coefficient (cm^2/s), A_0 = tracer input activity (Bq), F = cross section of the sample (cm^2), Φ = relative activity distribution.

The mean pixel values in the segments $F_{x,y}$ of the cross sections CS1 (position z) and CS2 (position $z+\Delta z$) are

$$A_{11} = \Phi(z,t) = \frac{K}{\sqrt{\sigma(t)}} \cdot \exp - \frac{(z-vt)^2}{\sigma} \tag{3}$$

$$A_{21} = \Phi(z+\Delta z,t) = \frac{K}{\sqrt{\sigma}} \exp - \frac{(z+\Delta z-vt)^2}{\sigma} \tag{4}$$

$$A_{22} = \Phi(z+\Delta z, t+\Delta t) = \frac{K}{\sqrt{\sigma\sqrt{1+\Delta t/t}}} \exp - \frac{(z+\Delta z - v(t+\Delta t))^2}{\sigma\sqrt{1+\Delta t/t}} \tag{5}$$

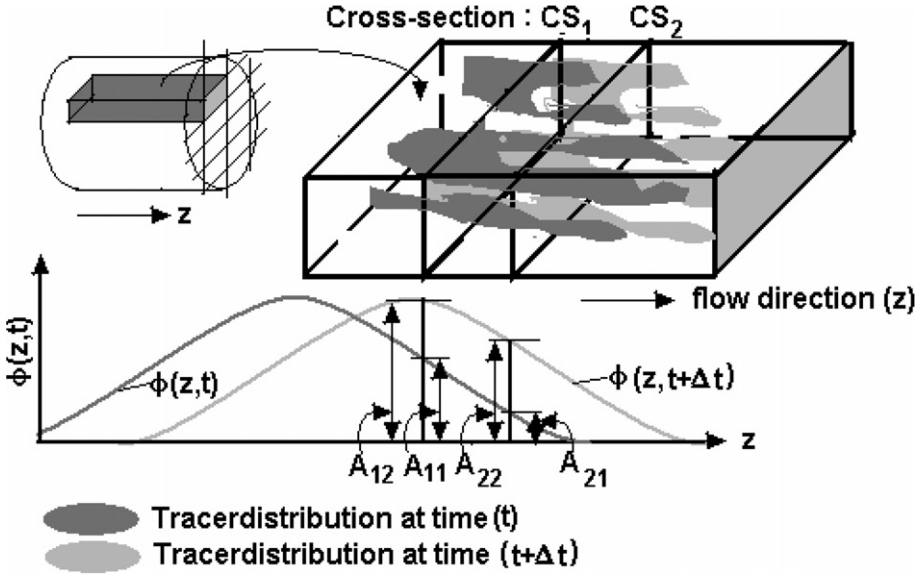

Fig. 2. Distribution of the tracer peak in the cross section segment at two times.

With Eqs. (3)–(5) the logarithmic concentration ratios for the segments F_{xy} can be calculated

$$\sigma \ln\left(\frac{A_{11}}{A_{21}}\right) = C_1 - 2C_2 v \tag{6}$$

$$\sigma \ln\left(\frac{A_{11}}{A_{22}}\right) - \frac{\ln C_3}{2} = C_4 - 2C_5 v + C_6 v^2 \tag{7}$$

$$C_1 = 2z\Delta z + (\Delta z)^2 \tag{8}$$

$$C_2 = 2\Delta z \cdot t \tag{9}$$

$$C_3 = (1 + \Delta t/t)^{1/2} \tag{10}$$

$$C_4 = z^2(1/C_3 - 1) + \frac{2z\Delta z + z^2}{C_3} \tag{11}$$

$$C_5 = zt(1/C_3 - 1) + \frac{t(z + \Delta z) + \Delta t \Delta z}{C_3} \tag{12}$$

$$C_6 = t^2(1/C_3 - 1) + \frac{2t\Delta t + (\Delta t)^2}{C_3} \tag{13}$$

With

$$A^* = \frac{\ln\left(\frac{A_{11}}{A_{22}}\right) - 1/2\ln(C_3)}{\ln\left(\frac{A_{11}}{A_{22}}\right)} \tag{14}$$

follows from (6) and (7) for the velocity v_{xy} in the segment F_{xy}

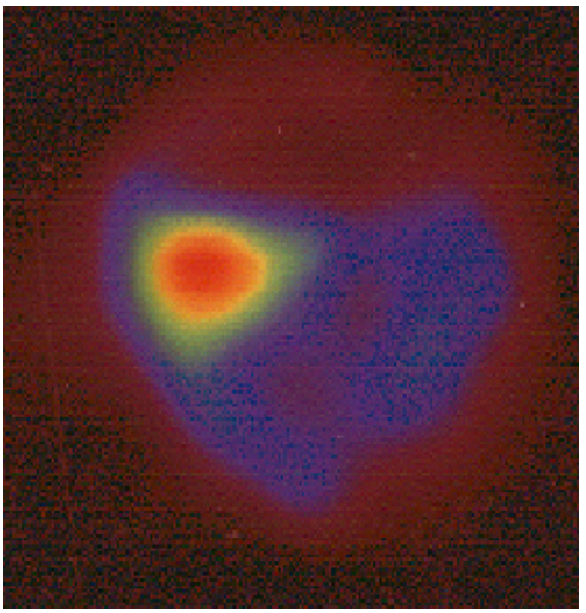

Fig. 3. Tracer concentration distribution in the drill core 7 min after injection, cross section 7.5 cm above the column bottom, KF-tracer concentration: red: 1.9–1.6 μg/cm^3, green: 1.6–1.3 μg/cm^3, blue: 1.3–1.0 μg/cm^3, dark red: < 1.0 μg/cm^3.

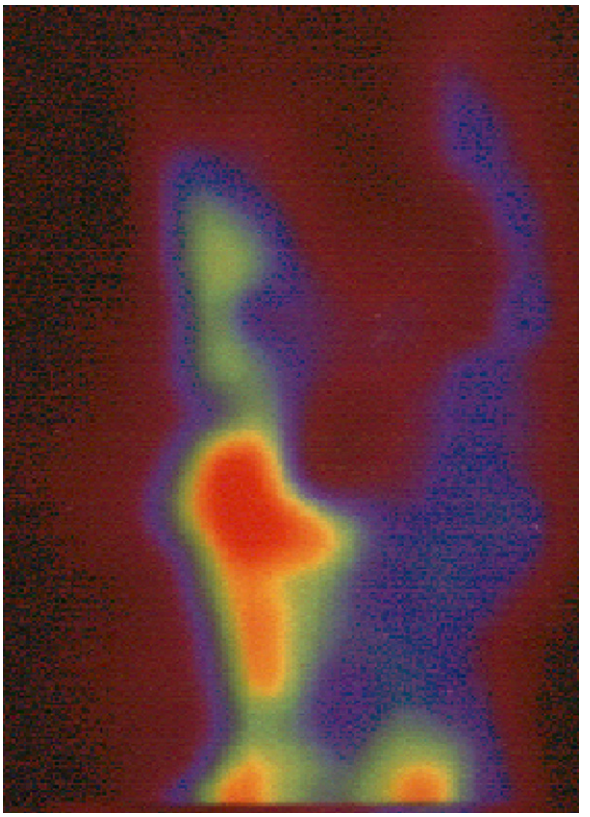

Fig. 4. Axial tracer distribution in the drill core 7 min after injection in the section 5–12 cm above the column bottom, KF-tracer concentration: red: 1.9–1.6 μg/cm^3, green: 1.6–1.3 μg/cm^3, blue: 1.3–1.0 μg/cm^3, dark red: <1.0 μg/cm^3.

$$v_{xy} = \frac{C_5 + C_2 A^*}{C_6} + \sqrt{\left(\frac{C_5 + C_2 A^*}{C_6}\right)^2 - \frac{C_5 + C_2 A^*}{C_6}} \tag{15}$$

Only ratios of the tracer concentration values have to be determined. It is not necessary to calibrate the pixel values for the reconstruction of absolute tracer concentration values.

The PET images of the water flow in the drill core of the lignite mining dump were evaluated on the basis of Eq. (15).

3.3. Calculation of the spatial distribution of hydrodynamic parameters using statistical moments

The spatial statistical moments are determined for several segments of the cross section, if a stack of cross section images was taken along the sample axis coordinate z during the PET measuring.

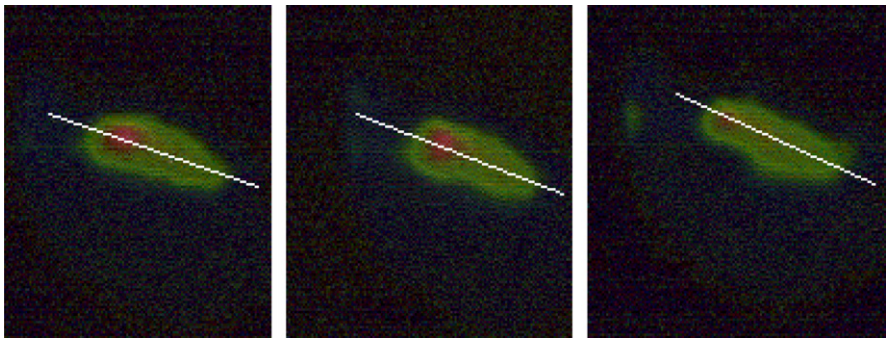

Fig. 5. Tracer distribution in the cross sections of the drill core, h = distance above the column bottom, T_i = time after tracer input, the colour index is the same as in Figs. 3 and 4: left: CS_1: $h = 46$ cm, $T_1 = 27$ min, middle: CS_1: $h = 46.5$ cm, $T_1 = 27$ min, right: CS_1: $h = 46.5$ cm, $T_2 = 32$ min.

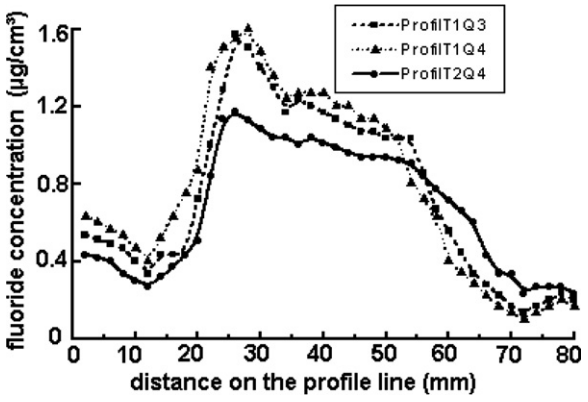

Fig. 6. Tracer concentration along the profile lines of Fig. 5.

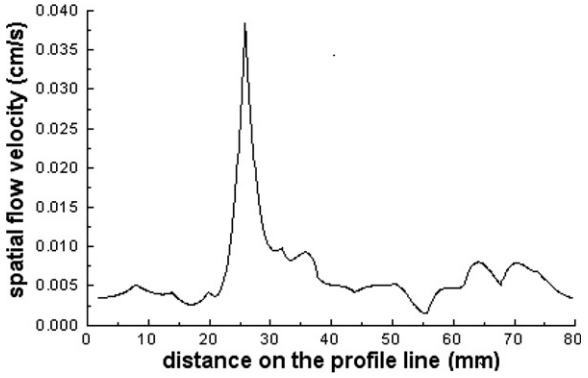

Fig. 7. Flow velocity distribution along the profile line of the drill core.

The following spatial moments $M_i(x,y,t)$ can be calculated with the mean density values $C_{xy}(z,t)$ of a cross section segment (x,y), determined in all images (z) of the stack measured at time t:

$$M_0(x,y,t) = \int_0^{Z_{\max}} C_{xy}(z,t)\mathrm{d}z \tag{16}$$

$$M_1(x,y,t) = \int_0^{Z_{\max}} C_{xy}(z,t)\cdot z\mathrm{d}z \tag{17}$$

$$M_2(x,y,t) = \int_0^{Z_{\max}} C_{xy}(z,t)\cdot z^2\mathrm{d}z \tag{18}$$

Generally the radial dispersivity α_r in porous layers is much lower than the axial dispersivity α_a ($\alpha_a \approx 20 \ldots 50\ \alpha_r$). In consideration of this relation the distribution of model parameters can be estimated approximately as follows:

Spatial distribution of flow velocity

$$v(x,y) = \frac{M_1(x,y,t_1)/M_0(x,y,t_1)}{t_1 - t_0} - \frac{M_1(x,y,t_0)/M_0(x,y,t_0)}{t_1 - t_0} \tag{19}$$

Spatial distribution of mass flow

$$M(x,y) = M_0(x,y)\cdot v(x,y) \tag{20}$$

Spatial distribution of axial dispersivity

$$\alpha_a(x,y) = \frac{M_2^*(x,y,t_1) - M_2^*(x,y,t_0)}{2(t_1 - t_0)\cdot v(x,y)} \tag{21}$$

with

$$M_2^*(x,y,t_1)_i = \frac{M_2^*(x,y,t_i)}{M_0^*(x,y,t_i)} - \left(\frac{M_1^*(x,y,t_i)}{M_0^*(x,y,t_i)}\right)^2 \tag{22}$$

Eqs. (16)–(22) were used for the quantitative evaluation of the PET studies of the Cu flow.

Eqs. (6)–(22) were derived particularly with regard to the modelling based on Darcy's law, the advection–dispersion approach and a voxel volume containing several pores. More specific and detailed

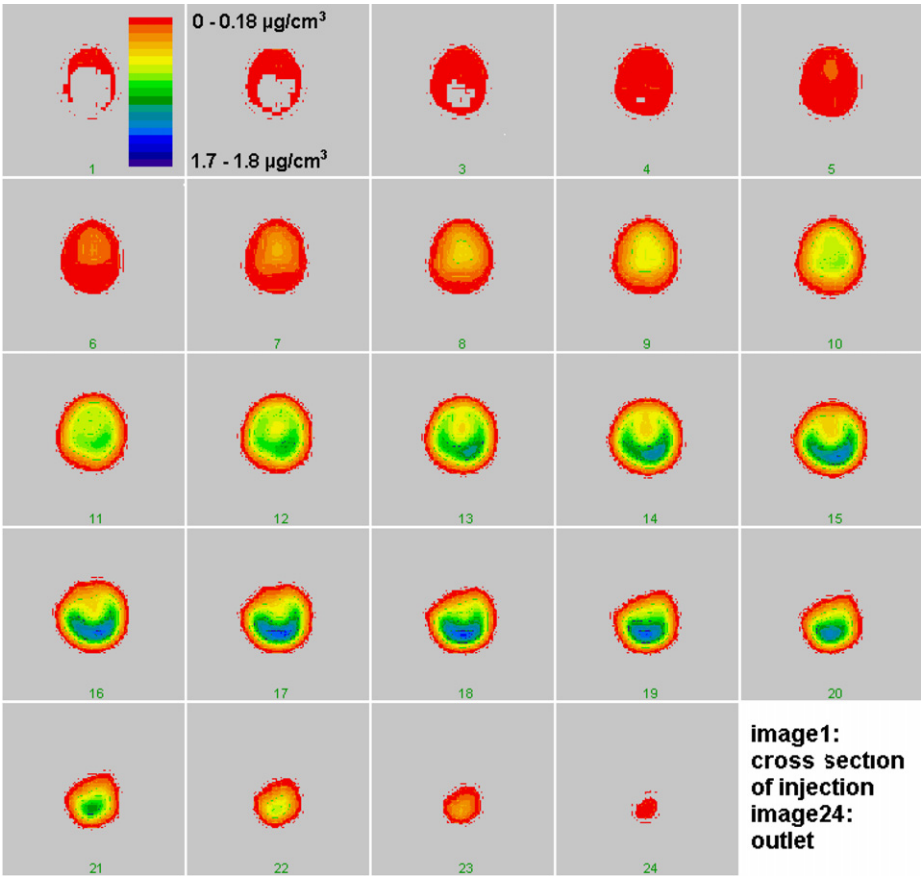

Fig. 8. Distribution of Cu ions in different cross sections, 440 s after tracer injection.

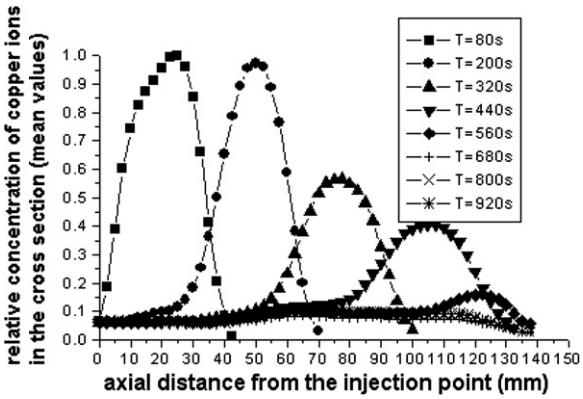

Fig. 9. Axial concentration profiles of Cu ions at different times.

micro-scale models have been developed in the last years which simulate the heterogeneous flow by means of the properties of the porous layer or the network of fractures (Bause and Knabner, 2004; Loggia et al., 2004; Vogel, 2000; Vogel and Roth, 2001; Xu and Hu, 2004). PET studies can also give important information for the verification and parameter estimation of these models. This will be a future field of the authors' activities.

4. Results and discussion

4.1. PET study of the spatial flow distribution in a drill core of the lignite mining dump

Residence time measurements in the drill core showed that one part of the water is passing the column very fast, the other part is passing slowly with a widely spread distribution. The tomographic images show impressively the reason for this phenomenon. Both images (Figs. 3 and 4) illustrate the existence of a main flow channel (red region). A lateral or diffusion flow results in a slow transport velocity in the vicinity of the main flow channel (blue region).

The spatial flow velocity distribution ($v(x,y)$) was calculated from the tracer concentration distribution

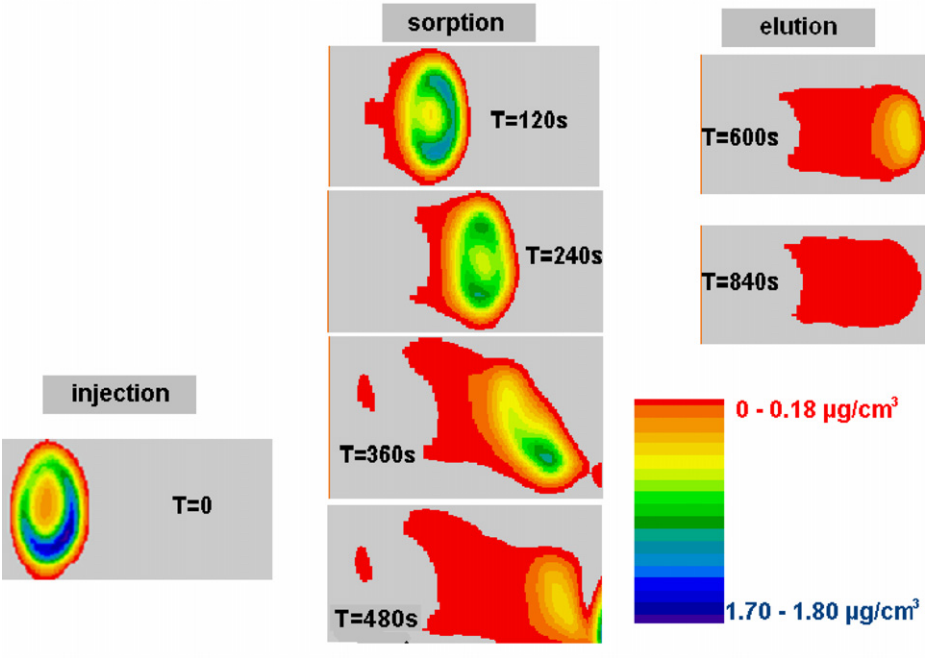

Fig. 10. Axial Cu concentration distribution in the vertical midplane (Fig. 1) of the horizontal column (concentration range: 0–1.8 µg/cm^3).

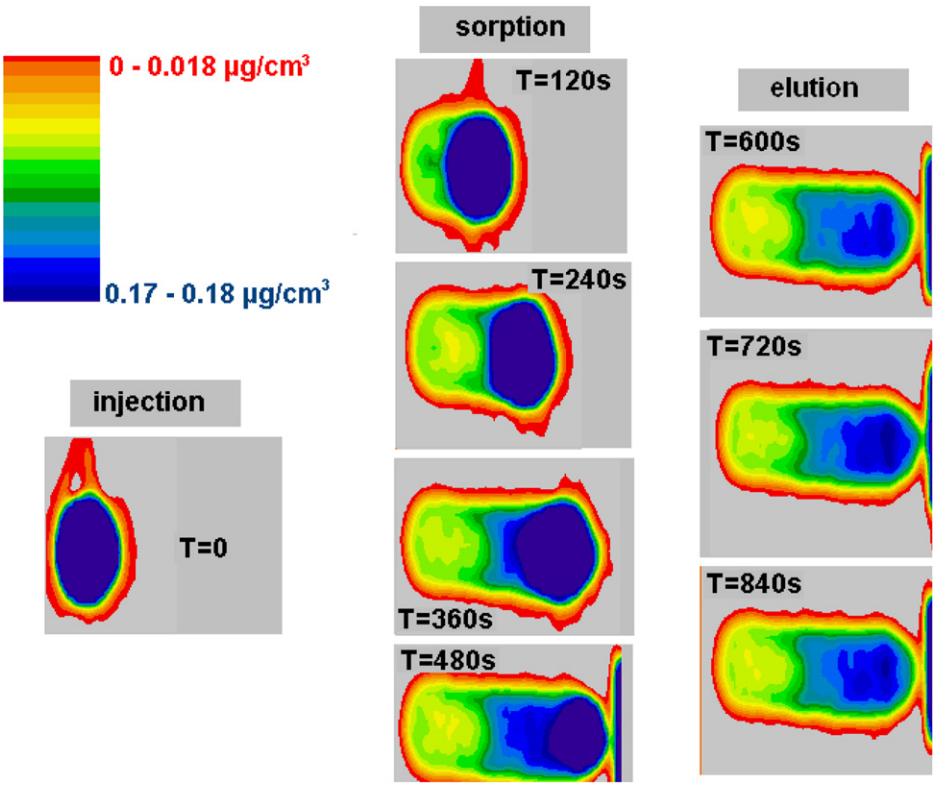

Fig. 11. Axial Cu concentration distribution in the vertical midplane (Fig. 1) of the horizontal column (lower concentration range: 0–0.18 µg/cm^3), no concentration decrease during the elution.

measured at two times ($t, t + \Delta t$) in two neighbouring cross sections (CS_1, CS_2, distance Δz) using Eq. (15). The tracer concentration distributions are determined from the tomographic images of two neighbouring cross sections (Fig. 5) along a profile line (Fig. 6). The velocity distribution calculated with the concentration profiles of Fig. 6 using Eq. (15) is shown in Fig. 7. The maximum velocity of 0.04 cm/s corresponds with the peak maximum in the conventional residence time distribution at the column outlet which was determined before the PET experiments.

4.2. Investigation of the transport of copper ions in a horizontal soil column

A typical example of the spatial Cu distribution in the cross section of the column measured 360 s after injection is shown in Fig. 8.

The other images of the sorption phase show a similar pattern. Spatial distribution curves are reconstructed by determination of the mean concentration values in the cross section (Fig. 9). The irreversibly adsorbed part of the Cu ions can be estimated from the area integrals of the curves. 27% of the Cu ions were adsorbed during the flow of the tracer impulse. The real water flow velocity calculated from the residence time distribution is 0.023 cm/s for a specific fluid input flow rate of 8.3×10^{-3} cm/s (effective porosity $\varepsilon = 0.36$). The velocity of the Cu impulse can be determined from the first moments of the curve in Fig. 9 to be 0.0226 cm/s. No retardation can be observed for the non irreversibly adsorbing part of the Cu ions because the velocity is nearly the same as the velocity of the conservative tracer (Br^-) used in the residence time measurements.

Figs. 10 and 11 show the axial distribution of Cu ions at different times displayed for different concentration ranges. Fig. 10 demonstrates the asymmetric flow in the horizontal column. Such asymmetric flow distribution was observed also with MRT studies of Cu transport in a similar column (Nestle et al., 2003a,b). It is caused probably by structure heterogeneities of the column filling. Fig. 11 shows the Cu concentration of the lower concentration range. There is no decrease during the elution process. This means that this part of the Cu is adsorbed strongly by the matrix. Equal concentrations were used in the MRT studies (Nestle et al., 2003a). But it was not possible to detect the concentration variations within the Cu plume with MRT. Still lower concentration distributions could be studied with PET using a radiotracer with higher specific activity.

These results show that PET measurements provide detailed information about the geochemical transport processes inside a geological matrix. Errors caused by unfavourable measurement conditions can be detected and eliminated in the parameter estimation and validation. Two PET image stacks measured at different times were combined and the spatial distribution of the model parameters was calculated with the statistical moment Eqs. (16)–(22) on the basis of a regular grid selection. The results are presented as profile plots (Figs. 12–14). The horizontal layering of the velocity was also measured with MRT tomography. The authors think it is an effect of the inhomogeneous structure of the sandy layer which was caused by the filling of the column in the horizontal position.

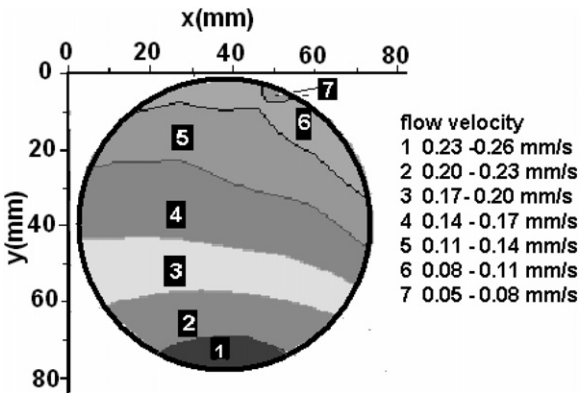

Fig. 12. Spatial distribution of the flow velocity in the cross section at the end of the horizontal column, 320 s after tracer injection.

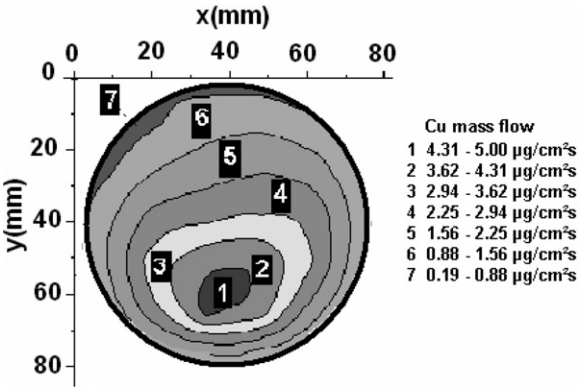

Fig. 13. Spatial distribution of mass flow of Cu ions in the cross section at the end of the horizontal column, 320 s after tracer injection.

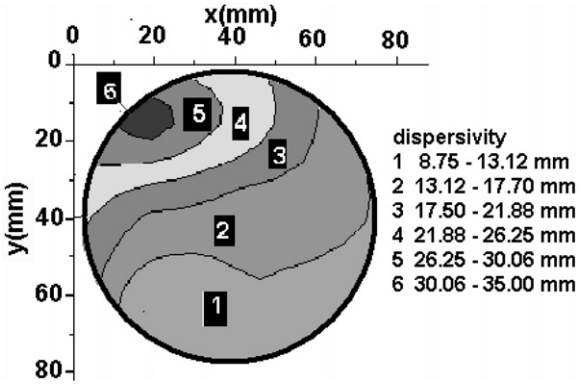

Fig. 14. Spatial distribution of axial dispersivity in the cross section at the end of the horizontal column, 320 s after tracer injection.

The large variation of the parameters in the cross section of the column demonstrates impressively the necessity for spatial resolved transport studies for modelling of geochemical transport processes and development of improved up-scaling methods.

Acknowledgements

This work has been supported by a grant from Bundesministerium für Wirtschaft und Arbeit (BMWA), Projektträger Wassertechnologie und Entsorgung, Projekt 02 E 9380 and by a grant from Deutsche Forschungsgemeinschaft, Projekt Ri 838/3. We thank Dr. D. Alber and P. Wolf of the Hahn-Meitner-Institut Berlin for Cu activation in the nuclear reactor, Dr. D. Lazik (UFZ Leipzig/Halle) for the preparation of the drill core of the lignite mining dump and Dr. N. Nestle (TU München, Institut für Hydrochemie) for the preparation of the horizontal soil column.

References

Bause, M., Knabner, P., 2004. Computation of variably saturated subsurface flow by adaptive mixed hybrid finite element methods. Adv. Water Res. 27, 565–581.

Bayer, A., Vogel, H.J., Roth, K., 2004. Direct measurement of soil water retention curve using X-ray absorption. Hydrol. Earth System Sci. 8, 2–7.

Clunie, D.A., 2000. Dicom-Structured Reporting. Pixel Med. Publ., Pensylvania.

Degueldre, C., Böck, H., Townsand, D., 1996. Porosity and pathway determination in crystalline rock by positron emission tomography and neutron radiography. Earth Planet. Sci. Lett. 140, 213–225.

Deuerer, M., Vogeler, I., 2004. Magnetic resonance imaging of hydrodynamic dispersion in a saturated porous medium. TIPM 54, 145–166.

Hall, L.D., Gao Amin, M.H., Dougherty, E., Sanda, M., Votruba, J., Richards, K.S., Chorley, J., Cislerova, M., 1997. MR properties or water in saturated soils and resulting loss of MRI signal in water content detection at 2 tesla. Geoderma 80, 431–448.

Kastel, R., Vogel, H.J., Roth, K., 2000. From lokal hydraulic properties to effective transport in soil. Eur. J. Soil Sci. 51, 91.

Loggia, D., Gouze, P., Greswell, R., Parker, D.J., 2004. Investigation of the geometrical dispersion regime in a single fracture using positron emission imaging. TIPM 55, 1–20.

Nestle, N., Baumann, T., Niessner, R., 2002. Magnetic resonance imaging in environmental science. Environ. Sci. Technol. 37, 154 A–160 A.

Nestle, N., Baumann, T., Wunderlich, A., Niessner, R., 2003a. MRI observation of heavy metal transport in aquifer matrices down to sub-mg quantities. Magnet. Resonance Imaging 21, 345–349.

Nestle, N., Wunderlich, A., Baumann, T., Niessner, R., 2003b. Spatial and temporal observations of adsorption and remobilisation of heavy metal ions in a sandy aquifer matrix using magnetic resonance imaging. Environ. Sci. Technol. 37, 3972–3977.

Ogilvie, S.R., Orribo, J.M., Glower, P.W.J., 2001. The influence of deformation bands upon fluid flow using profile permeatry and positron emission tomography. Geophys. Res. Lett. 28, 61–64.

Oswald, S., Kinzelbach, W., Greiner, A., Brix, G., 1997. Observation of flow processes in artificial porous media via magnetic resonance imaging in three dimensions. Geoderma 80, 417–429.

Oswald, S., Schneidegger, B., Kinzelbach, W., 2002. Time-dependent measurement of strongly density-dependent flow in a porous medium via nuclear magnetic resonance imaging. TIPM 47, 169–193.

Rasband, W., Bright, D., 1995. NIH Image: a public domain image processing program for Macintosh. Microbeam. Anal. 4.

Richter, M., 2002. Concepts for modelling of heterogeneous flow processes in soil columns on the basis of tomographic radiotracer experiments. In: Schulz, H.D., Teutsch, G. (Eds.), Geochemical Processes – Conceptual Models for Reactive Transport in Soil and Groundwater. Wiley-VCH, Weinheim, pp. 20–38.

Richter, M., Gründig, M., Butz, T., 2000. Tomographische Radiotracerverfahren zur Untersuchung von Transport- und Sorptionsprozessen in geologischen Schichten. Zeitschr. Angew. Geologie 46, 1001–1009.

Van As, H., van Dusschoten, D., 1997. NMR methods for imaging of transport processes in micro-porous systems. Geoderma 80, 389–403.

Vogel, H.J., 2000. A numerical experiment on pore size, pore connectivity, water retention, permeability, and solute transport using network models. Eur. J. Soil Sci. 51, 99–105.

Vogel, H.J., Roth, K., 2001. Quantitative morphology and network representation of soil pore structure. Adv. Water Res. 24, 233–242.

Vogel, H.J., Bastian, P., Roth, K., 1999. Downscaling hydrodynamischer Eigenschaften zur Schätzung von Transportprozessen. Mitt. Dtsch. Bodenkundl. Ges. 91, 278–281.

Xu, J., Hu, B., 2004. A numerical Eularian method of moment for solute transport in a nonstationary dual-porosity medium. Adv. Water Res. 27, 207–222.